fields in producing power absorption in various subjects differs according to their sizes.

References

[1] C. C. Johnson and A. W. Guy, "Nonionizing electromagnetic wave effects in biological materials and systems," *Proc. IEEE*, vol. 60, pp. 692–718, June 1972.
[2] S. M. Michaelson, "Human exposure to nonionizing radiant energy—Potential hazards and safety standards," *Proc. IEEE*, vol. 60, pp. 389–421, Apr. 1972.
[3] A. S. Pressman, *Electromagnetic Fields and Life* (translated from Russian). New York: Plenum, 1970.
[4] K. Martha, J. Musil, and H. Tuha, *Electromagnetic Fields and the Environment* (translated from Czech). San Francisco, Calif.: San Francisco Press, 1971.
[5] "Biological effects and health implications of microwave radiation," in *Symp. Proc.*, S. F. Cleary, Ed., BRH–DBE 70-2, U. S. Department of Health, Education, and Welfare, Rockville, Md., Sept. 17–19, 1969.
[6] *IEEE Trans. Microwave Theory Tech.* (*Special Issue on Biological Effects of Microwaves*), vol. MTT-19, pp. 128–257, Feb. 1971.
[7] R. A. Tell, "Broadcast radiation: How safe is safe?" *IEEE Spectrum*, vol. 9, pp. 43–51, Aug. 1972.
[8] H. R. Kucia, "Accuracy limitations in measurements of HF field intensities for protection against radiation hazards," *IEEE Trans. Instrum. Meas.* (*1972 Conference on Precision Electromagnetic Measurements*), vol. IM-21, pp. 412–415, Nov. 1972.
[9] S. J. Rogers, "Radio frequency radiation hazards to personnel at frequencies below 30 MHz," in *Symp. Proc. Biological Effects and Health and Implications of Microwave Radiation* (Richmond, Va.), Sept. 17–19, 1969, pp. 222–232.
[10] H. P. Schwan, "Biological hazards from exposure to ELF electrical fields and potentials," U. S. Naval Weapons Lab., Tech. Rep. TR-2713, Mar. 1972.
[11] J. A. Stratton, *Electromagnetic Theory*. New York: McGraw-Hill, 1941, sec. 9.25.
[12] A. W. Guy, C. C. Johnson, J. C. Lin, A. F. Emery, and K. K. Kraning, "Electromagnetic power deposition in man exposed to HF fields and the associated thermal and physiological consequences," Univ. Washington School of Medicine, Dep. Rehabilitation Medicine, Seattle, Sci. Rep. 1, Mar. 1973.

Characterization of Nonlinearities in Microwave Devices and Systems

GEORGE L. HEITER, MEMBER, IEEE

Invited Paper

***Abstract*—A simple model to describe a nonlinear device or system is proposed which extends the power series expansion, conventionally restricted to amplitude nonlinearities, to include phase nonlinearities as well. Four different test methods are selected for which the experimentally observed nonlinearity parameters are related to the "gain" and "phase" coefficients of the extended series. A set of simplified relationships is derived where the "1-dB gain compression point" represents gain contributions only while phase nonlinearities are included in the "intercept point," the "third-order intermodulation (IM) coefficients," and the "noise-power-ratio (npr)." For a TWT amplifier in which phase nonlinearities dominate, the third-order IM coefficient was measured. The results are compared with those calculated from single-tone and noise-loading tests using the relationships derived from the model. Agreement to ±1 dB is found over a 15-dB power range.**

I. Introduction

With microwave devices and systems utilized ever closer to their limits, linear measurement techniques are no longer sufficient to describe final performance under multisignal loading conditions. As a result, a number of techniques have evolved which are used to characterize nonlinear behavior and the resulting intermodulation (IM) performance. Selection of a particular technique depends on the type of information desired, such as detailed diagnostic information on the origin of nonlinearity, overall IM performance under different loading conditions, etc. Four of these techniques—single-tone, two-tone, three-tone testing, and noise loading—were discussed at a panel session [1] on which this paper is based.

Some of the present microwave techniques have been adapted from the CATV industry [1, p. 112], [3] where the IM performance at UHF frequencies has been a primary concern for about two decades. There it has been found that the reliability of IM testing for system evaluation increases as the probing signal spectrum approaches that of the actual system load.

The usefulness of tests with probing signals which have a spectral distribution different from that of the final system load depends in part on how closely the selected mathematical model approaches actual device behavior. The Volterra series expansion [3]–[6] allows detailed and accurate representation of device characteristics, including memory, which can be applied directly to any spectral distribution of the system load. Measurement [6] of the relevant parameters (kernels), however, is sometimes time consuming and may exceed available measurement capabilities.

In this paper a simple mathematical model is proposed which is used to describe the amplitude and phase nonlinearities (gain deviation and AM–PM conversion) observed in microwave devices. From this model the parameters relevant to each of the four measurement techniques are derived and interrelated (equation numbers of simplified relationships are marked □ for convenient reference). For each technique

Manuscript received August 14, 1973; revised August 29, 1973.
The author is with Bell Laboratories, North Andover, Mass. 01845.

a representative experimental setup is shown schematically, and the limitations of the measured parameters are discussed. For a selected device [a traveling wave tube (TWT)], predicted and observed parameters are compared.

II. The Model

Selection of a model [2]–[10] was based on combining analytical simplicity with experimental convenience in determining parameter values to represent both amplitude and phase nonlinearities. Such a model can be constructed by extending the conventional amplitude power series expansion [2], [11] to include order-dependent time delays (Fig. 1). For the case when time delays of all orders are equal, this model reduces to the conventional amplitude model; for unequal time delays, power-level-dependent phase shifts are introduced. Consider, for example, the total output in the fundamental band. It consists of the output due to the linear term ("linear output") and the fundamental components of all odd-order terms. Relative to the linear output, these have in-phase and quadrature-phase components where the angle of their vector sum depends on the time-delay differences.

The time-dependent voltage transfer function between the input and output of the device is, therefore, written as

$$e_o(t) = c_0 + c_1 e_i(t - t_1) + c_2 e_i^2(t - t_2) + c_3 e_i^3(t - t_3) + \cdots \quad (1)$$

where

- $e_o(t)$ instantaneous output voltage [V];[1]
- $e_i(t)$ instantaneous input voltage [V];
- c_j series expansion coefficient of order j $[V^{-j+1}]$;
- t_j time delay of the jth-order term [s].

Here c_j is assumed to be independent of frequency and power level. All time-delay differences are referenced to the delay of the linear output

$$\Delta t_j = t_j - t_1. \quad (2)$$

In many practical cases devices operate with less than octave bandwidth. Since even-order terms in (1) will produce distortion products which fall outside this band, subsequent discussions will neglect all even-order terms. Only inband IM components produced by odd-order terms will be considered.

III. Single-Tone Test

Although this test is not now widely used, it provides a simple means of separating amplitude and phase nonlinearity contributions and allows estimating the IM performance under more complicated loading conditions. The accuracy of this estimate depends on how closely (1) models the device; good agreement has been found, for example, in TWT amplifiers.

In the single-tone test, the device is excited with

$$e_i(t) = A \cos(\alpha t + \phi_0) \quad (3)$$

where A equals peak input voltage [V] and $\phi_0 = 0$ from selection of input reference plane. With only odd-order terms retained in (1), this results in an output voltage of

$$e_o(t) = c_1 A \cos \alpha(t - t_1) + c_3 A^3 \cos^3 \alpha(t - t_3) + \cdots. \quad (4)$$

[1] Dimensions are denoted by square brackets throughout.

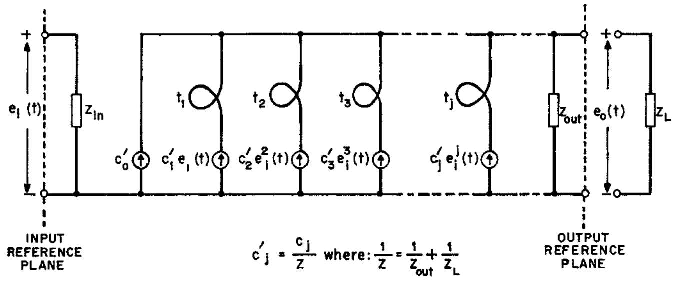

Fig. 1. Model of nonlinearity.

If all output measurements are referenced to the time-delayed ($\tau_D = t_1$) input signal, we can set $t_1 = 0$. Using trigonometric identities and collecting equal frequency terms, the output voltage at frequency $n\alpha$ can be written as

$$e_{on\alpha}(t) = A_{n\alpha} \cos n\alpha t + B_{n\alpha} \sin n\alpha t, \qquad n = \text{odd}. \quad (5)$$

It is convenient to write the amplitudes $A_{n\alpha}$ and $B_{n\alpha}$ of the in-phase and quadrature-phase components of (5) in terms of new gain and phase coefficients a_j and b_j. At frequency $n\alpha$ these are related to the coefficients c_j of (1) by

$$\left.\begin{aligned} a_j^{(n\alpha)} &= c_j \cos(n\alpha \Delta t_j) \\ b_j^{(n\alpha)} &= c_j \sin(n\alpha \Delta t_j) \end{aligned}\right\} \qquad n, j = \text{odd}. \quad (6)$$

Using (2) and with $t_1 = 0$, the fundamental and third-harmonic amplitudes become

$$A_\alpha = a_1^{(\alpha)} A + \frac{3}{4} a_3^{(\alpha)} A^3 + \frac{5}{8} a_5^{(\alpha)} A^5 + \frac{35}{64} a_7^{(\alpha)} A^7 + \cdots \quad (7a)$$

$$B_\alpha = b_1^{(\alpha)} A + \frac{3}{4} b_3^{(\alpha)} A^3 + \frac{5}{8} b_5^{(\alpha)} A^5 + \frac{35}{64} b_7^{(\alpha)} A^7 + \cdots \quad (7b)$$

$$A_{3\alpha} = \frac{1}{4} a_3^{(3\alpha)} A^3 + \frac{5}{16} a_5^{(3\alpha)} A^5 + \frac{21}{64} a_7^{(3\alpha)} A^7 + \cdots \quad (8a)$$

$$B_{3\alpha} = \frac{1}{4} b_3^{(3\alpha)} A^3 + \frac{5}{16} b_5^{(3\alpha)} A^5 + \frac{21}{64} b_7^{(3\alpha)} A^7 + \cdots. \quad (8b)$$

Note that from the above assumptions

$$a_1^{(\alpha)} = c_1 \qquad b_1^{(\alpha)} = 0. \quad (9)$$

For the present test, only the fundamental output is considered ($n = 1$); in subsequent discussions the superscript (α) in (6), (7), and (9) is omitted for convenience. For the fundamental component, (5) can be written as

$$e_{o\alpha}(t) = (\hat{e}_{o\alpha}) \cos(\alpha t + \phi_\alpha) \quad (10)$$

where

$$\hat{e}_{o\alpha} = \sqrt{A_\alpha^2 + B_\alpha^2} \approx A_\alpha \quad (11a)$$

$$\phi_\alpha = \arctan \frac{B_\alpha}{A_\alpha} \approx \frac{B_\alpha}{A_\alpha}. \quad (11b)$$

The approximations in (11) are valid at sufficiently low power levels or high gains where $A_\alpha \gg B_\alpha$ (since $b_1 = 0$), which in many devices extends into the region where gain changes can readily be observed.

Single-tone tests are conveniently performed in a bridge-type circuit (Fig. 2). The CW source is low-frequency modu-

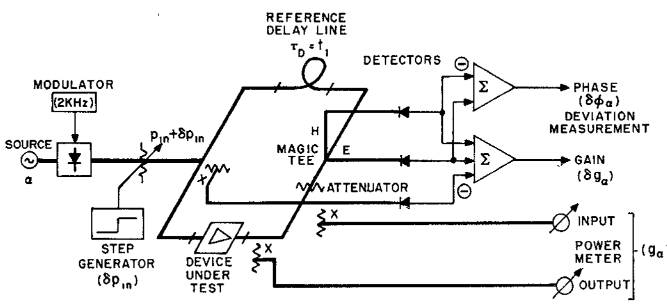

Fig. 2. Schematic circuit for single-tone nonlinearity measurement.

lated (for example, at 2 kHz) to allow accurate phase measurements to be made at the modulating frequency. A step-driven p-i-n diode modulator follows, which generates input power level changes δp_{in}. The resulting changes in insertion gain and phase of the device under test, δg_α and $\delta\phi_\alpha$, are detected using the sum and difference outputs from the E- and H-arms of the magic T. The advantage of fast input power stepping [12] is that very small gain and phase changes can be observed without critical requirements on frequency and temperature stability since the bridge can be balanced just prior to the application of each step. Also, thermal and instantaneous changes in transmission properties can be distinguished. The input and output power meters measure absolute gain g_α. Frequently, dynamic range limitations in the detection circuitry require additional attenuation (or gain with known IM properties) in the test arm to compensate for high gains (or losses) in the device under test. For a device with $Z_{\text{in}} = Z_{\text{out}} = R$ [Ω], the input and fundamental output power levels are from (3), (10), and (11)

$$p_{\text{in}} = \left(\frac{A}{\sqrt{2}}\right)^2 \frac{10^3}{R} \qquad [\text{mW}] \tag{12a}$$

$$p_{\text{out}\,\alpha} \equiv p_\alpha \approx \left(\frac{A_\alpha}{\sqrt{2}}\right)^2 \frac{10^3}{R} \qquad [\text{mW}]. \tag{12b}$$

The gain coefficients a_j of (6) can be found from power measurements by curve fitting (7a) to a plot of A_α versus A using (12). The sign of a_3 determines the nature of the amplitude nonlinearity: It is called "expansive" for $a_3 > 0$ and "compressive" for $a_3 < 0$.

Most practical devices are compressive and therefore frequently specified [13] in terms of the 1-dB gain compression point $p_{\alpha,1\,\text{dB}}$, which is the output power level where $A_\alpha/a_1A = 0.89$. For a third-order device (a_j, $b_j = 0$, for $j > 3$) with sufficient gain such that the approximation of (11a) holds, and with the low-level power gain given by

$$G_0 = 20 \log_{10}(a_1) \qquad [\text{dB}] \tag{13}$$

an estimate of $|a_3|$ can be obtained from (7) and (12); for $R = 50\ \Omega$ and using capital letters for logarithmic (dB) notation throughout

$$\begin{aligned} P_{\alpha,1\,\text{dB}} &= 10 \log_{10}(p_{\alpha,1\,\text{dB}}) \\ &= G_0 - 10 \log_{10}\left(\frac{|a_3|}{a_1}\right) + 0.62 \quad [\text{dBm}]. \end{aligned} \tag{14}$$

The phase coefficients b_j of (7) can be found using a series of input power steps δp_{in} [mW] (Fig. 2), and measuring the corresponding phase changes $\delta\phi_\alpha$ [deg], of the fundamental output signal. The results can be fitted to an expansion of the form

$$\begin{aligned} k_\alpha &\equiv \frac{\delta\phi_\alpha}{\delta p_\alpha \times 10^{-3}} \\ &= k_0 + k_1\left(\frac{p_\alpha}{10^3}\right) + k_2\left(\frac{p_\alpha}{10^3}\right)^2 + \cdots \ [°/\text{W}] \end{aligned} \tag{15}$$

such that from (6), (11), and (12), and with $k_j' = (\pi/180)k_j$

$$\begin{aligned} b_3 &= \frac{4}{3}\left(\frac{A_\alpha}{A}\right)^3 \frac{1}{2R} k_0' \\ b_5 &= \frac{8}{5}\left(\frac{A_\alpha}{A}\right)^5 \left(\frac{1}{2R}\right)^2 k_1' \\ &\ \ \vdots \end{aligned} \tag{16}$$

The factor 10^3 is included in (15) to conform to the more conventional definition of the AM–PM conversion coefficient k_α in degrees/watt of output power. Note that for third-order devices operated in the region where $A_\alpha \approx a_1A$

$$k_\alpha = k_0 \propto \frac{\frac{\pi}{180}\phi_\alpha - \alpha t_1}{A^2} \approx \frac{3}{4}\frac{b_3}{a_1} = \text{constant} \tag{17}$$

is independent of power level and thus a convenient measure of the phase nonlinearity of a device over a wide range of output power levels.

The frequency dependence of the nonlinearity parameters can be evaluated by varying α over the desired band.

IV. Two-Tone Test

This method uses one of the inband IM products to describe the device nonlinearity in terms of the intercept point [14], [15]. The advantage over the single-tone test is that the sum of gain and phase nonlinearities is evaluated directly. Measurements are made in or near the frequency range of interest at amplitudes which exceed those of the third-harmonic output.

The device is excited by two (conventionally equal-level) tones

$$e_i(t) = A(\cos \alpha t + \cos \beta t). \tag{18}$$

From (1) this results in an output spectrum of the form

$$e_o(t) = \sum_{m=-\infty}^{\infty} \sum_{n=-\infty}^{\infty} e_{n\alpha+m\beta}(t) \tag{19}$$

where, as in (5)

$$\begin{aligned} e_{n\alpha+m\beta}(t) \\ = A_{m,n} \cos(n\alpha + m\beta)t + B_{m,n} \sin(n\alpha + m\beta)t \end{aligned} \tag{20}$$

with amplitudes

$$A_\alpha = a_1{}^{(\alpha)}A + \frac{9}{4} a_3{}^{(\alpha)}A^3 + \frac{25}{4} a_5{}^{(\alpha)}A^5 + \cdots \tag{21a}$$

$$A_\beta = a_1{}^{(\beta)}A + \frac{9}{4} a_3{}^{(\beta)}A^3 + \frac{25}{4} a_5{}^{(\beta)}A^5 + \cdots \tag{21b}$$

$$A_{2\alpha\pm\beta} = \frac{3}{4} a_3^{(2\alpha\pm\beta)} A^3 + \frac{25}{8} a_5^{(2\alpha\pm\beta)} A^5 + \cdots \qquad (21c)$$

$$A_{3\alpha} = \frac{1}{4} a_3^{(3\alpha)} A^3 + \frac{25}{16} a_5^{(3\alpha)} A^5 + \cdots \qquad (21d)$$

and corresponding expressions for $B_{m,n}$. As in (6), the gain and phase coefficients are

$$\left.\begin{aligned} a_j^{(n\alpha+m\beta)} &= c_j \cos(n\alpha + m\beta)\Delta t_j \\ b_j^{(n\alpha+m\beta)} &= c_j \sin(n\alpha + m\beta)\Delta t_j \end{aligned}\right\} (m+n), \; j = \text{odd} \qquad (22)$$

with output amplitude, phase, and power levels as in (10)–(12).

The intercept point is found experimentally from either individual tone or total power measurements. Here, the former method is selected where the input and output power levels of one of the exciting tones (for example, $p_{\text{in},\alpha}$ and p_α) and one of the IM products (for example, $p_{2\alpha-\beta}$) are measured [Fig. 3(a)]. The input power level p_{in} from the two CW sources (α and β) set to equal levels is controlled by the input attenuator and monitored by the input power meter. The fundamental output power level is measured using a bandpass filter (BPF) with bandwidth $B < |\alpha - \beta|/2$ around the center frequency α. A second BPF with the same bandwidth around the center frequency $2\alpha - \beta$ and a power meter measure the selected IM product. A high-quality isolator has to precede this filter to absorb the reflected fundamental power. The results are plotted [Fig. 3(b), solid lines] on logarithmic scales (for example, in dBm). The intercept point is then defined as that output power level P_I [dBm] at which $P_{2\alpha-\beta}$ [dBm] would intercept P_α [dBm] if low-level results were extrapolated [Fig. 3(b), dashed lines] into the high-power region.

To relate P_I to the coefficients of (22), assume that the test frequencies are selected such that $\alpha \approx \beta \approx (2\alpha - \beta)$; therefore

$$a_j^{(\alpha)} \approx a_j^{(\beta)} \approx a_j^{(2\alpha-\beta)} \equiv a_j \qquad (23a)$$

$$b_j^{(\alpha)} \approx b_j^{(\beta)} \approx b_j^{(2\alpha-\beta)} \equiv b_j. \qquad (23b)$$

Then, by the definition of the extrapolations, the small angle approximations of (11) hold and $A_\alpha = a_1 A$ such that from (12), (21), and (22)

$$p_\alpha = \left(\frac{a_1 A}{\sqrt{2}}\right)^2 \frac{10^3}{R} \quad [\text{mW}] \qquad (24a)$$

$$p_{2\alpha-\beta} = \left(\frac{1}{\sqrt{2}} \frac{3}{4} A^3 \sqrt{a_3^2 + b_3^2}\right)^2 \frac{10^3}{R} \quad [\text{mW}]. \qquad (24b)$$

Since at p_I by definition $p_\alpha = p_{2\alpha-\beta}$

$$p_I = \frac{2}{3} a_1^2 \left(\frac{a_1}{\sqrt{a_3^2 + b_3^2}}\right) \frac{10^3}{R} \quad [\text{mW}] \qquad (25a)$$

or, for $R = 50\ \Omega$ and using (13)

$$\begin{aligned} P_I &= 10 \log_{10} p_I \\ &= G_0 + 10 \log_{10} \left(\frac{a_1}{\sqrt{a_3^2 + b_3^2}}\right) \\ &\quad + 11.25 \quad [\text{dBm}]. \end{aligned} \qquad \boxed{(25b)}$$

Note that if P_I were defined in terms of the total power levels (i.e., $p_\alpha + p_\beta$), then the intercept point would shift to $P_I' = P_I + 4.52$ dBm.

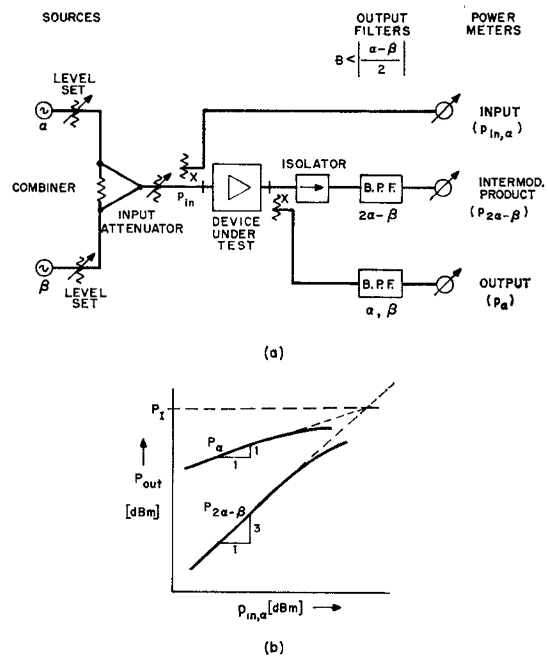

Fig. 3. Two-tone nonlinearity test. (a) Schematic measurement circuit. (b) Definition of the intercept point.

A relationship between P_I and $P_{\alpha,1\text{ dB}}$ can be found from (14) and (25); for third-order devices in which $a_3 \gg b_3$

$$P_I = P_{\alpha,1\text{ dB}} + 10.6 \quad [\text{dBm}]. \qquad \boxed{(26)}$$

Note, however, that in many practical devices these assumptions are not valid. Note, also, that because of the difference in constants between (7) and (21), the 1-dB gain compression point found from a two-tone test and measuring total power output, $P^{(2)}_{\text{total},1\text{ dB}}$, is related to (14) by

$$P^{(2)}_{\text{total},1\text{ dB}} = P_{\alpha,1\text{ dB}} - 1.76 \quad [\text{dBm}]. \qquad (27)$$

From (25) it is seen that p_I is independent of p_{in}; the intercept point is, therefore, a useful measure of the total device nonlinearity. From its knowledge and in the power region where a given device follows the extrapolation, the IM level is related to P_α by

$$P_{2\alpha-\beta} = 3P_\alpha - 2P_I \quad [\text{dBm}]. \qquad (28)$$

Caution has to be exercised, however, when these conditions are not met, for example, when amplitude or frequency-dependent linearization techniques are used [15], [16]. When cascading devices, the final device requires the highest P_I. Assume that there is no interaction between nonlinearities of neighboring devices (such as cancellation of phase contributions). Then from (25) the intercept point of the cascade is approximately equal to the intercept point of the final device if the intercept points of successive devices differ by less than the gain of each stage.

V. Three-Tone Test

Here, again, specific inband IM products are selected to characterize overall device nonlinearities, commonly through the third-order intermodulation coefficient [9], [11], [17].

The more even spectral distribution and flexibility while still allowing discrete frequency evaluation make this an attractive test for multifrequency (such as communication) systems.

In this test three (equal-level) tones are applied to the input

$$e_i(t) = A(\cos \alpha t + \cos \beta t + \cos \gamma t) \tag{29}$$

yielding from (1) an output spectrum of the form

$$e_o(t) = \sum_{l=-\infty}^{\infty} \sum_{m=-\infty}^{\infty} \sum_{n=-\infty}^{\infty} e_{n\alpha+m\beta+l\gamma} \tag{30}$$

where

$$e_{n\alpha+m\beta+l\gamma} = A_{l,m,n} \cos (n\alpha + m\beta + l\gamma)t + B_{l,m,n} \sin (n\alpha + m\beta + l\gamma)t \tag{31}$$

with amplitudes

$$A_\alpha = a_1^{(\alpha)} A + \frac{15}{4} a_3^{(\alpha)} A^3 + \frac{155}{8} a_5^{(\alpha)} A^5 + \cdots \tag{32a}$$

$$A_{\alpha\pm\beta\pm\gamma} = \frac{3}{2} a_3^{(\alpha\pm\beta\pm\gamma)} A^3 + \frac{45}{4} a_5^{(\alpha\pm\beta\pm\gamma)} A^5 + \cdots \tag{32b}$$

$$A_{2\alpha\pm\beta} = \frac{3}{4} a_3^{(2\alpha\pm\beta)} A^3 + \frac{55}{8} a_5^{(2\alpha\pm\beta)} A^5 + \cdots \tag{32c}$$

$$A_{2\alpha\pm2\beta\pm\gamma} = \frac{15}{8} a_5^{(2\alpha\pm2\beta\pm\gamma)} A^5 + \cdots \tag{32d}$$

$$A_{3\alpha} = \frac{1}{4} a_3^{(3\alpha)} A^3 + \frac{45}{16} a_5^{(3\alpha)} A^5 + \cdots \tag{32e}$$

$$\vdots \qquad \vdots$$

and corresponding expressions for $B_{l,m,n}$. For brevity, only one expression for each type of output amplitude is given in (32). Corresponding expressions can be found by permutation of α, β, and γ.

The coefficients of order j are given by

$$\left.\begin{aligned} a_j^{(n\alpha+m\beta+l\gamma)} &= c_j \cos (n\alpha + m\beta + l\gamma)\Delta t_j \\ b_j^{(n\alpha+m\beta+l\gamma)} &= c_j \sin (n\alpha + m\beta + l\gamma)\Delta t_j \end{aligned}\right\}$$

$$(l + m + n),\ j = \text{odd}. \tag{33}$$

In terms of the output power levels, defined as in (12), the third-order intermodulation coefficient is defined [11] as

$$m_x \equiv \frac{p_x}{p_\alpha p_\beta p_\gamma} \bar{p}^2 \tag{34a}$$

where

$\bar{p} = 1$ mW = normalization factor;

p_x= measured output power level of the IM product at frequency x (e.g., 3α, $\alpha+\beta-\gamma$, etc.).

Second- or higher order IM coefficients with similar properties can be defined by analogy [11]. Note that if a third-order device is operated in the low-power region ($A_\alpha \approx a_1 A$), then m_x is independent of power level and thus a convenient measure of overall device nonlinearity. For the equal-level excitation (34a) can be written in logarithmic form as

$$M_x = 10 \log_{10} m_x = P_x - 3P_\alpha \quad [\text{dB}] \tag{34b}$$

since $10 \log_{10} \bar{p} = 0$ dBm. With the assumption that in this test the narrow-band approximation of (23) still holds, the IM coefficients associated with the individual inband product frequencies are related from (32) by

$$M_{\alpha+\beta-\gamma} = M_{2\alpha-\beta} + 6 = M_{3\alpha} + 15.56 \text{ [dB]}. \tag{35}$$

The highest $(\alpha+\beta-\gamma)$-type product is frequently selected [17] for measuring M in a circuit of the type shown in Fig. 3(a). However, because of the more complex output spectrum in the region of the fundamental band of (30) as compared to (19), simple filtering of tones may not be sufficient to yield accurate results. Other techniques [5, fig. 5] (such as linear output tone cancellation [18]) may have to be employed.

From (12), (23), (32), and (34), $m_{\alpha+\beta-\gamma}$ is related to the gain and phase coefficients in a third-order device (a_j, $b_j=0$, for $j>3$) by

$$m_{\alpha+\beta-\gamma} = \left(\frac{3\bar{p}}{a_1^2 p_{\text{in}}}\right)^2 (\mathcal{A}_3^2 + \mathcal{B}_3^2) \cdot \left[\frac{1}{\left(1+\frac{5}{2}\mathcal{A}_3\right)^2 + \left(\frac{5}{2}\mathcal{B}_3\right)^2}\right]^3 \tag{36}$$

where $p_{\text{in}} = 3p_{\text{in},\alpha}$ equals total input power, and

$$\mathcal{A}_3 \equiv \frac{a_3}{a_1} \frac{p_{\text{in}}R}{10^3} \qquad \mathcal{B}_3 \equiv \frac{b_3}{a_1} \frac{p_{\text{in}}R}{10^3}. \tag{37}$$

At low input power levels where $\mathcal{A}_3$, $\mathcal{B}_3 \ll 1$, the last bracket of (36) becomes unity and

$$m_{\alpha+\beta-\gamma} = \left(\frac{a_3^2 + b_3^2}{a_1^2}\right)\left(\frac{3\bar{p}R}{10^3 a_1^2}\right)^2 \tag{38a}$$

or, with (13) and for $R = 50\ \Omega$

$$M_{\alpha+\beta-\gamma} = 10 \log_{10} \left(\frac{a_3^2 + b_3^2}{a_1^2}\right) - 2G_0 - 16.5 \quad [\text{dB}]. \tag{38b}$$

With these assumptions, $M_{\alpha+\beta-\gamma}$ can therefore be calculated from the gain and phase coefficients measured in a single-tone test. Introducing $\oplus$ for "power addition" such that

$$10 \log_{10} \left(\frac{a_3^2 + b_3^2}{a_1^2}\right) = \left[10 \log_{10} \left(\frac{a_3}{a_1}\right)^2\right] \oplus \left[10 \log_{10} \left(\frac{b_3}{a_1}\right)^2\right] \tag{39}$$

then from (14) and (17)

$$M_{\alpha+\beta-\gamma} = [-2P_{\alpha,1\,\text{dB}} - 15.3] \oplus [20 \log_{10} k_0 - 89.1] \quad [\text{dB}]. \tag{40a}$$

Also, from (25b) and (38b)

$$M_{\alpha+\beta-\gamma} = -2P_I + 6 \quad [\text{dB}]. \tag{40b}$$

Note that when devices are cascaded and if there is no interaction between nonlinearities, the IM coefficient translates from (38b) with twice the gain of each section, whereas both $P_{a,1\text{ dB}}$ and P_I translate directly with gain (or loss).

When the low-level approximation does not hold, it is seen from (36) and (37) that M becomes unsymmetrical in a_3 and b_3 and depends on the sign of a_3; for example, for a given $|a_3|$ the value of M differs between expansive and compressive devices.

VI. Noise Loading

In this test [7], [11], [19], [20] the input signal is obtained from a "white" noise source which is band limited to the instantaneous frequency range of interest. The nonlinearity to be measured is then given in terms of the noise-power-ratio (npr), which relates the "signal" noise output to the IM noise generated by all nonlinearities. For signals whose spectral distribution can be approximated by that of white noise, this test method is used commercially [19] to evaluate the IM performance of complete systems.

Let $S_i(f)$, the input power spectral density of the zero-mean Gaussian noise source, be a constant N_i over the selected bandwidth $2\Delta f$ around the center frequency f_0 [Fig. 4(a)]. Kuo [21] has shown that if (1) is extended to the Jth order, and with the narrow-band assumptions of (23), then the autocorrelation function of the output signal is given by

$$R_{\text{out}}(\tau) = \sum_{n=0}^{J} (A_n + B_n) R_{\text{in}}^n(\tau). \tag{41a}$$

Here

$$A_n = \frac{1}{n!}\left[\sum_{m=0}^{L} \frac{(n+2m)!\,a_{n+2m}}{2^m m!} R_{\text{in}}^m(0)\right]^2 \tag{41b}$$

with a similar expression for B_n, and

$$L = \begin{cases} \dfrac{J-n}{2}, & \text{for } J-n \text{ even} \\ \dfrac{J-n-1}{2}, & \text{for } J-n \text{ odd} \end{cases}$$

$$R_{\text{in}}(\tau) \equiv \overline{e_i(t)e_i(t+\tau)} \qquad \text{(statistical average)} \tag{41c}$$

$$R_{\text{in}}(0) \equiv \int_{-\infty}^{\infty} S_i(f)\,df = 4\Delta f N_i$$

$$= p_{\text{in}}^{(N)} \frac{R}{10^3} \equiv p \tag{41d}$$

where $p_{\text{in}}^{(N)}$, defined as in (12), is the average "signal" noise input power, and p is defined for notational convenience. The Fourier transform of (41a) then yields the signal output power spectral density $S_o(f)$.

To find the IM noise output, a very narrow portion of the input spectrum, $\delta f \ll \Delta f$ (Fig. 4a), is removed ("notch" [11], "dark band" [19]). Then, the major contribution to the output power within the notch is due to nonlinearities. With the notch placed at $f=f_o$, the npr is defined as

$$\text{npr} \equiv \frac{S_o(f_o)}{S_{on}(f_o)} \tag{42}$$

where $S_{on}(f_o)$ is $S_o(f_o)$ with the notch in place. Kuo [21] has shown that (for $J=5$ and $b_1=0$)

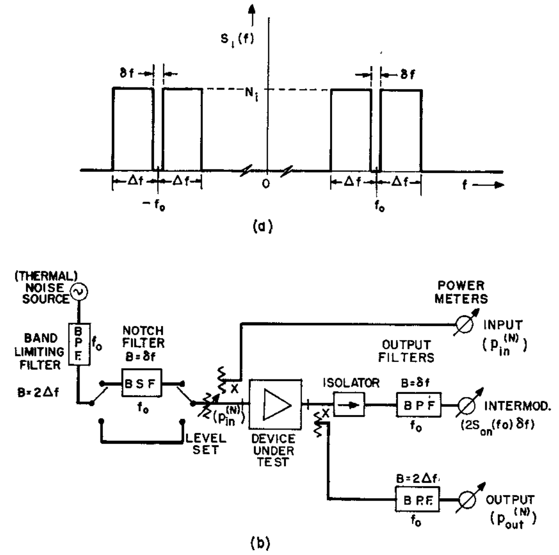

Fig. 4. Noise-loading test. (a) Signal noise input power density spectrum. (b) Schematic measurement circuit.

$$\begin{aligned} S_o(f_o) = {} & (a_1 + 3a_3p + 15a_5p^2)^2 N_i + (3b_3p + 15b_5p^2)^2 N_i \\ & + 6[(a_3 + 10a_5p)^2 + (b_3 + 10b_5p)^2](\tfrac{3}{4}p)^2 N_i \\ & + \frac{2875}{64}(a_5^2 + b_5^2)p^4 N_i \end{aligned} \tag{43a}$$

and, if the notch is sufficiently narrow, Kuo [21] has shown that for the case when the notch is in place

$$\begin{aligned} S_{on}(f_o) \approx {} & 6[(a_3 + 10a_5p)^2 + (b_3 + 10b_5p)^2](\tfrac{3}{4}p)^2 N_i \\ & + \frac{2875}{64}(a_5^2 + b_5^2)p^4 N_i. \end{aligned} \tag{43b}$$

From (42) and (43)

$$\text{npr} \approx 1 + \frac{(a_1+3a_3p+15a_5p^2)^2+(3b_3p+15b_5p^2)^2}{\frac{27}{8}[(a_3+10a_5p)^2+(b_3+10b_5p)^2]p^2+\frac{2875}{64}(a_5^2+b_5^2)p^4}. \tag{44}$$

As long as the narrow-band approximations are valid, (44) predicts the input power dependence of npr for a set of gain and phase coefficients which can be found from a single-tone test. A typical npr measurement circuit [11], [19], [20], [5, fig. 11] [Fig. 4(b)] uses an output power meter preceded by a BPF with a bandwidth equal to or slightly less than that of the bandstop filter (BSF), which introduces the notch. For a given input power level, the npr then is the ratio of the intermodulation power meter readings with and without the notch in place. Power level and gain (or loss) measurements are obtained from the input and output power meter readings. The purpose of the isolator is the same as in Fig. 3(a).

Consider now a third-order device (a_j, $b_j=0$, for $j>3$). Then, for p/a_1 small, (44) can be rewritten using (37) as

$$\text{npr} = \frac{11}{3} + \frac{16}{9}\frac{1}{\mathcal{A}_3} + \frac{8}{27}\left(\frac{1}{\mathcal{A}_3^2 + \mathcal{B}_3^2}\right). \tag{45}$$

As expected, npr$\rightarrow\infty$ as a_3, $b_3\rightarrow 0$, that is, as the device approaches linearity. For small values of $\mathcal{A}_3$, $\mathcal{B}_3$ (that is, low power levels or high gains), (45) can be approximated by

$$\text{npr} \approx \frac{8}{27}\left(\frac{10^3}{R}\right)^2 a_1^2 \left(\frac{1}{a_3^2 + b_3^2}\right)\left(\frac{1}{p_{\text{in}}^{(N)}}\right)^2, \quad \text{for npr} > 10^3 \tag{45a}$$

and thus (npr) $(p_{\text{in}}^{(N)})^2$ approaches the "noise constant" n_r, which is characteristic of a given device; in logarithmic notation, with (13) and for $R = 50\ \Omega$

$$N_r \equiv 10 \log_{10}(n_r) = \text{NPR} + 2P_{\text{in}}^{(N)} \quad [\text{dB}]$$
$$= G_0 + 10 \log_{10}\left(\frac{1}{a_3^2 + b_3^2}\right) + 20.74 \quad [\text{dB}] \tag{45b}$$

where, from (41d)

$P_{\text{in}}^{(N)} = 10 \log_{10} p_{\text{in}}^{(N)}$
= average "signal" noise input power [dBm]
NPR = 10 $\log_{10}$ (npr) [dB].

This approximation can be used to find simple relationships between npr of (45a), $m_{\alpha+\beta-\gamma}$ of (38), and p_I of (25) if it is assumed that the corresponding total average input power levels ($p_{\text{in}}^{(N)}$, $3p_{\text{in},\alpha}$, and $2p_{\text{in},\alpha}$, respectively) are equivalent. Then

$$P_I = G_0 + \tfrac{1}{2}(\text{NPR} + 2P_{\text{in}}^{(N)}) + 0.87 \quad [\text{dBm}] \tag{46a}$$

and

$$M_{\alpha+\beta-\gamma} = -(\text{NPR} + 2P_{\text{in}}^{(N)}) - 2G_0 + 4.26 \quad [\text{dB}]. \tag{46b}$$

As $\mathcal{A}_3$ and $\mathcal{B}_3$ increase further, (45) has to be used. The selection of sign for the roots of the quadratic equation (45) depends again, as in (36) for $m_{\alpha+\beta-\gamma}$, on the character of the nonlinearity, that is, on whether the device is expansive or compressive. In this region gain deviations can no longer be neglected. As in (41d) the total inband "signal" noise power output $p_o^{(N)}$ is given by

$$p_o^{(N)} \frac{R}{10^3} = R_o(0) \approx \sum_{f_o-\Delta f}^{f_o+\Delta f} S_o(f)df \approx 2S_o(f_o)(2\Delta f). \tag{47a}$$

From (37) and (43a) this becomes

$$p_o^{(N)} = a_1^2 p_{\text{in}}^{(N)} \left[1 + 6\mathcal{A}_3 + \frac{99}{8}(\mathcal{A}_3^2 + \mathcal{B}_3^2)\right] \quad [\text{mW}] \tag{47b}$$

which, together with (45) and (36), defines the correspondence between $m_{\alpha+\beta-\gamma}$ and npr. For convenience, the deviation $\Delta M_{\alpha+\beta-\gamma}$ [dB] from the asymptotic expression (46b) is plotted as a function of NPR in Fig. 5.

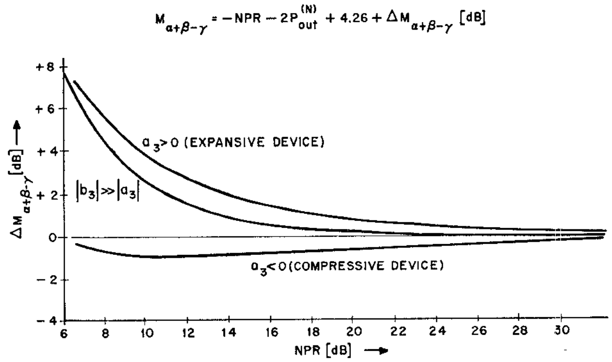

Fig. 5. Relation between $M_{\alpha+\beta-\gamma}$ and NPR for third-order nonlinearities with correction curves for low values of NPR when either gain deviations ($a_3>0$, $a_3<0$) or phase deviations ($|b_3| \gg |a_3|$) dominate.

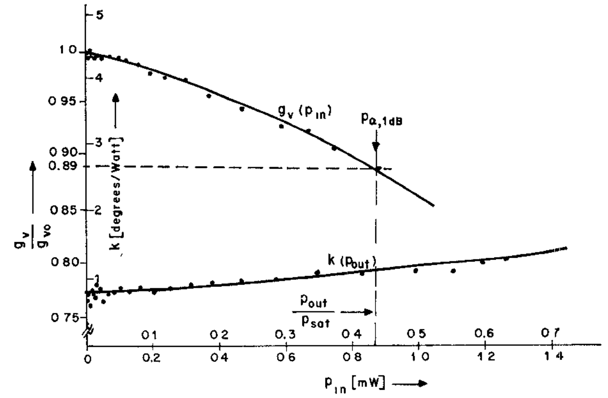

Fig. 6. Curve fitting (to fifth order) of single-tone measurements on a traveling-wave tube.

TABLE I

SINGLE-TONE GAIN AND PHASE COEFFICIENTS

j=	0	1	3	5	7
a_j	0	158.95	-283	-2.45×10^3	-1.28×10^4
k_j	0.81	2.45×10^{-2}	1.26×10^{-3}	0	0
b_j	0	0	757.0	6.95×10^3	5.64×10^4

VII. Comparison with Experimental Results

The validity of the model and the resulting conversion equations were evaluated for the case of a TWT amplifier. Three sets of measurements were performed over a relative bandwidth of $2\Delta f/f_o = 0.5$ percent as a function of power level:

1) a single-tone test [12] at band center;
2) a three- (equal-level) tone test [22] with two frequencies (α and γ) located at the band edges, and the third frequency (β) located $\Delta f/5$ from the lower band edge;
3) a noise-loading test [20], [23] with a 10-dB notch width of $\Delta f/200$ located at center band.

The gain and phase coefficients in (6) are extracted from curve fitting the single-tone test results to (7) and (15). The results are used in (36), (45), and (47b) to predict $M_{\alpha-\beta+\gamma}$ and NPR. These predictions are then compared with the results of experiments 2) and 3).

In the single-tone test [12], the input power level was stepped in 1-dB increments over a power range of approximately 30 dB. At the output, the level of the fundamental tone P_α [dBm], the change in power gain δG_α [dB], and the change of insertion phase $\delta\phi_\alpha$ [deg] were recorded for each step. For $R = 50\ \Omega$, the voltage gain $g_v(p_{\text{in}})$ and the AM–PM conversion coefficient $k(p_{\text{out}})$ were calculated. To the resulting points polynomials were fitted (Fig. 6) from which the single-tone coefficients were obtained (Table I).

Over the same dynamic range, a set of three-tone tests [17], [22] was performed (Fig. 7, open circles). In the output power range between +18 dBm and +30 dBm, $M_{\alpha-\beta+\gamma}$ is found to be constant. At higher power levels $|M_{\alpha-\beta+\gamma}|$ decreases due to compression of p_α. This is consistent with the single-tone test observations: The major contribution to the observed behavior arises from AM–PM conversion as seen

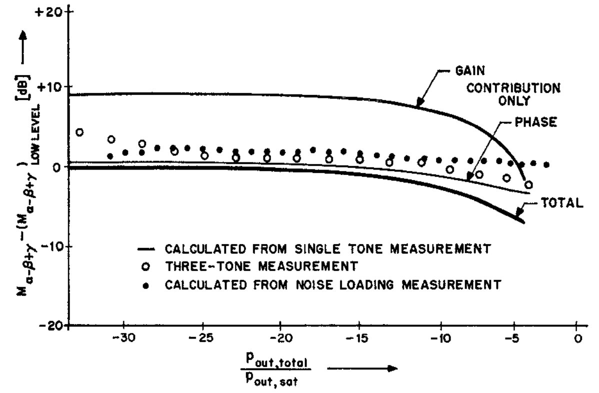

Fig. 7. Comparison of three-tone measurement results with $M_{\alpha-\beta+\gamma}$ calculated from single-tone and noise-loading measurements using the conversion relations derived from the model.

from the curves (solid lines in Fig. 7) calculated from Table I, and using (36) to fifth order and inserting either gain or phase contributions (a_j or b_j) only. These two contributions add on a power basis from (39) to form the total predicted power dependence of $M_{\alpha-\beta+\gamma}$ (heavy line). For power levels below +18 dBm, $|M_{\alpha-\beta+\gamma}|$ is found to increase. This trend is also observed in the decrease of $k(p_{\text{out}})$ at low levels (Fig. 6) but not taken into account by the present model. This behavior can be included, however, into an extended, coupled-mode model where the initial mode saturates at an appropriately low power level.

Noise-loading tests [20] were limited in the low-power region by low S/N ratios and at high power levels by low values of NPR [20], [23]. However, approximately the same dynamic range as in the earlier measurements was covered. The results were translated to $M_{\alpha-\beta+\gamma}$ values using (45) and (47), and are also shown in Fig. 7 (solid points). Over most of the dynamic range, the NPR and $M_{\alpha-\beta+\gamma}$ measurements agree to better than ±0.5 dB. Although low NPR correction (Fig. 5) was applied, the agreement at levels above the 1-dB gain compression point is not as good. This is attributed to higher order deviations. At low levels the S/N ratio limitations are believed to be responsible for the observed deviations.

VIII. Conclusions

When characterizing the IM performance of devices or systems, it is important to consider both amplitude and phase nonlinearities. A simple mathematical model representing both contributions is used to interrelate IM parameters obtained from four measurement techniques of varying complexity.

The single-tone test uses a bridge circuit to evaluate gain and phase nonlinearities separately. Because of the simple and well-defined nature of the signal, this test allows detailed characterization of the frequency and power level dependence of nonlinearities. The result is a set of gain and phase coefficients up to the desired order of approximation. When limited to third order and power levels well below saturation, the 1-dB gain compression point $P_{1\text{ dB}}$ [dBm], together with the AM–PM conversion constant k[°/W] represent good estimates of IM performance.

The two-tone test uses narrow BPF's to find the output power scattered into the selected IM product frequency by both gain and phase nonlinearities simultaneously. Measurements are made at low input power levels and extrapolated to the intercept point P_I [dBm] between the fundamental and IM output power levels. For third-order nonlinearities, P_I is a convenient constant to compare IM performance of devices; when used in system design considerations, care has to be exercised to ensure that the extrapolations are still valid in the operating power range. This problem can be overcome by defining a two-tone third-order IM coefficient analogous to the one defined for three-tone tests.

The three-tone test requires improved filtering and/or signal tone cancellation to measure the power output at the selected IM product. The more even spectral distribution of the test signal over the desired band makes this test attractive for evaluating performance under multifrequency loading conditions. The third-order intermodulation coefficient M_3 [dB] characterizes the sum of gain and phase nonlinearities. For third-order devices, M_3 is a constant over a wide dynamic range; since it can be measured directly at the operating power level, it is a convenient measure for both device characterization and system design.

Noise loading uses a narrow BSF to remove a very small fraction (notch) from the band-limited white noise input spectrum. The power scattered into the notch is measured at the output to find the noise-power-ratio, NPR [dB], which characterizes the total IM performance. For third-order nonlinearities, the noise constant N_r [dB] is independent of power level over a wide dynamic range and, therefore, a convenient measure for both device and system performance under noiselike loading conditions.

Selection of a nonlinearity test method depends on the testing purpose: For detailed device characterization, the single-tone test yields the most specific diagnostic information; for device comparisons, the constants P_I, M_3, and N_r are desirable; for system design, as was found in the CATV industry, test results become more reliable as the test signal spectrum approaches that of the system load. When devices are cascaded and if interactions between nonlinearities can be neglected, the influence of each section on overall performance can be evaluated. This is accomplished by referring the constants to the output of the cascade using the insertion gain (or loss) between the section and cascade outputs, raised to the appropriate power.

Acknowledgment

The author wishes to thank the panel [1] members: K. A. Simons, F. F. Fulton, R. C. Heidt, J. C. Gillespie, as well as R. B. Swerdlow, for their valuable comments and results on the various measurement techniques, and Y. L. Kuo for making the results of his noise-loading analysis available prior to publication. The author also wishes to thank H. Miedema and R. E. Markle for their encouragement and many helpful discussions, E. F. Cook for his careful measurements, and S. Narayanan and J. Goldman for their critical review of the manuscript.

References

[1] Panel Session on "Nonlinearities in microwave devices and systems," in *Digest 1973 IEEE G-MTT Int. Microwave Symp.* (Boulder, Colo.), June 4–6, 1973, pp. 111 *ff.*
[2] K. Simons, *Technical Handbook for CATV Systems*, Jerrold Electronics Corp., Horsham, Pa.
[3] S. Narayanan, "Transistor distortion analysis using Volterra series representation," *Bell Syst. Tech. J.*, May–June, 1967.
[4] J. Goldman, "A Volterra series description of cross-talk interference in communications systems," *Bell Syst. Tech. J.*, vol. 52, pp. 649–668, sec. II, 1973.
[5] E. Bedrosian and S. O. Rice, "The output properties of Volterra

systems (nonlinear systems with memory) driven by harmonic and Gaussian inputs," *Proc. IEEE*, vol. 59, pp. 1688–1707, Dec. 1971.
[6] "Communication receiver interference modeling," in *Proc. 1972 IEEE Int. Conf. Communications*, June 19–21, 1972, Session 30.
[7] A. L. Berman and C. E. Mahle, "Nonlinear phase shift in traveling-wave tubes as applied to multiple access communications satellites," *IEEE Trans. Commun. Technol.*, vol. COM-18, pp. 37–48, Feb. 1970.
[8] O. Shimbo, "Effects of intermodulation, AM–PM conversion, and additive noise in multicarrier TWT systems," *Proc. IEEE* (*Special Issue on Satellite Communications*), vol. 59, pp. 230–238, Feb. 1971.
[9] H. C. Poon, "Modeling of bipolar transistor using integral charge-control model with application to third-order distortion studies," *IEEE Trans. Electron Devices*, vol. ED-19, pp. 719–731, June 1972.
[10] I. Tanaka *et al.*, "Nonlinear distortion and second harmonics in traveling-wave tubes," *Electron. Commun. Japan*, vol. 55B, pp. 62–68, 1972.
[11] *Transmission Systems for Communications*, 4th ed., Bell Labs., 1970, ch. 10.
[12] E. F. Cook, private communication, 1973.
[13] "Thin film on sapphire amplifier improves performance, is smaller," *Microwaves*, Aug. 1970.
[14] F. C. McVay, "Don't guess the spurious level," *Electron. Des.*, vol. 3, pp. 70–73, Feb. 1, 1967.
[15] F. F. Fulton, "Two-tone nonlinearity testing, the intercept point, P_I," Panel Session on "Nonlinearities in microwave devices and systems," in *Digest 1973 IEEE G-MTT Int. Microwave Symp.* (Boulder, Colo.), June 4–6, 1973, p. 112.
[16] ——, private communication, 1973.
[17] R. C. Heidt, "Three-tone nonlinearity testing—The intermodulation coefficient, M," Panel Session on "Nonlinearities in microwave devices and systems," in *Digest 1973 IEEE G-MTT Int. Microwave Symp.* (Boulder, Colo.), June 4–6, 1973, p. 113.
[18] H. Seidel, "A microwave feed-forward experiment," *Bell Syst. Tech. J.*, vol. 50, pp. 2879–2916, fig. 17, Nov. 1971.
[19] J. C. Gillespie, "Noise loading of FM systems—The noise-power-ratio, NPR, and customer requirements," Panel Session on "Nonlinearities in microwave devices and systems," in *Digest 1973 IEEE G-MTT Int. Microwave Symp.* (Boulder, Colo.), June 4–6, 1973, p. 113.
[20] R. B. Swerdlow, "Pseudo-random noise loading for system evaluation," Panel Session on "Microwave noise measurement and system effects," in *Digest 1973 IEEE G-MTT Int. Microwave Symp.* (Boulder, Colo.), June 4–6, 1973, p. 227.
[21] Y. L. Kuo, "Noise loading analysis of memoryless nonlinearity characterized by a Taylor series of finite order," to be published.
[22] R. C. Heidt, private communication, 1973.
[23] R. B. Swerdlow, private communication, 1973.

Broad-Band Microwave Measurements on GaAs «Traveling-Wave» Transistors

RAYMOND H. DEAN, MEMBER, IEEE, ARTHUR B. DREEBEN, JOHN J. HUGHES, MEMBER, IEEE, RALPH J. MATARESE, AND LOUIS S. NAPOLI, MEMBER, IEEE

***Abstract*—Instantaneous gain, noise figure, reverse attenuation, and gain and phase control measurements in the frequency range 8–18 GHz have been performed on GaAs traveling-wave transistors. The broad-band high-gain nature of the device together with the requirement for several bias connections precluded the use of standard test fixtures, and resulted in a package design exhibiting less than 1-dB insertion loss over the band together with 75- to 90-dB internal isolation. Untuned *X*-band gain, noise figure, and reverse attenuation were 12 dB, 18 dB, and 32 dB, respectively, and the gain and phase could be electronically varied over a 35-dB and 360° range. When RF tuning was employed, the gain, on the average, improved by 10 dB.**

I. Introduction

In 1967 Robson *et al.* [1] published a concise description of a two-port amplifier that made special use of the growing space-charge waves which travel unidirectionally from cathode to anode in a slab of n-type GaAs biased above the transferred-electron threshold. The high internal gain and built-in isolation made the device potentially attractive, but the use of closely compensated bulk material forced the authors to use pulsed biasing and placed constraints on the geometry which limited the net gain to several decibels and made the gain fall off rapidly above a few gigahertz.

Manuscript received May 14, 1973; revised July 12, 1973. This work was supported by the Air Force Avionics Laboratory, Wright-Patterson AFB, Ohio, under Contract F33615-72-C1616.

The authors are with the RCA Corporation, Princeton, N. J.

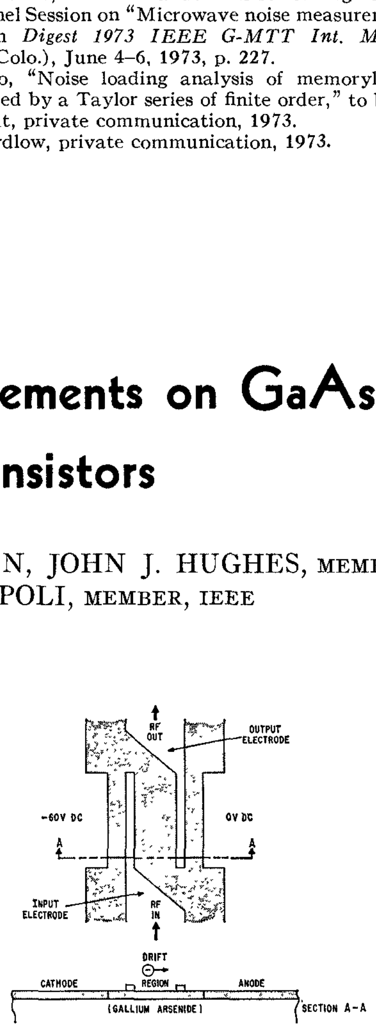

Fig. 1. Schematic of initial RCA traveling-wave transistor.

In 1970 Dean *et al.* [2] fabricated a similar device using 2-μm-thick epitaxially grown n-on-insulating GaAs. Because of the use of purer epitaxial material, dc biasing could be employed, and a more favorable geometry was obtained (see Fig. 1). The geometry employed in the epitaxial device resulted in significant unidirectional net gain in X band (8–12 GHz). The RF coupling electrodes on this device acted as Schottky-barrier electrodes, and in subsequent work, described in a 1972 paper by Dean and Matarese [3], it was shown that the input portion of the device behaved very much like a field-effect transistor. An EM wave propagating on the input line, shown in Fig. 1, produces a voltage. This voltage drives a conduction current, which establishes a fluc-